

Dielectric properties of CB@TiO₂/BaTiO₃/epoxy composites

Xin Wang¹ · Zewei Li¹

Received: 1 September 2016 / Accepted: 21 December 2016 / Published online: 14 February 2017
© Springer Science+Business Media New York 2017

Abstract High-k (High permittivity) dielectric composites with low dielectric loss exhibit great potential applications in embedded capacitors and energy storage systems. In this study, CB@TiO₂ core-shell particles and BaTiO₃ powder were incorporated into the epoxy matrix to fabricate three-phase composites. Morphology of CB@TiO₂ particles and dielectric properties of CB@TiO₂/BaTiO₃/epoxy composites were investigated. Results showed that the dielectric properties of the composites can be improved by the addition of CB@TiO₂ particles. The dielectric constant of the composites with 30 vol% BaTiO₃ and 20 vol% CB@TiO₂ can reach 32.14 at the frequency of 1 kHz while the dielectric loss (tanδ) of the composites still keeps low (0.016 at 1 kHz). Additionally, the positive effect of surface coating on the application of conductive filler is indicated by the results.

1 Introduction

Ferroelectric/polymer composites with high dielectric constant have enormous potential in electrical energy storage. Various high permittivity ferroelectric ceramics, such as BaTiO₃, PbTiO₃, SrTiO₃ and CaCu₃Ti₄O₁₂(CCTO), have been employed as fillers for high-k composites [1–4]. In order to achieve composites with improved dielectric constant, the content of ferroelectric ceramics powder should be higher. However, excessively high loading of filler can

deteriorate mechanical properties and processing performance of material [5, 6]. Therefore, improving the dielectric constant while remaining the concentration of ceramics particles is the target on achieving desirable material with better dielectric properties.

In recent years, one of the trends in this area is to incorporate conductive nanoparticles or fibers into the ferroelectric/polymer two-phase composites. According to the percolation theory, dielectric constant of conductor/polymer has an abrupt increase when the content of conductive filler is close to percolation threshold [7, 8]. Thus ferroelectric/conductor/polymer three-phase composites possess higher permittivity than ferroelectric/polymer two-phase composites. Nevertheless, some conductive fillers are liable to aggregate in the polymer matrix and lead to a high dielectric loss which definitely limits the application of composites [9].

Several methods like surface oxidation and surface modification have been tried to reduce the dielectric loss which cause by the agglomeration of conductive nanoparticles. However, to prevent conductive particles to contact with each other directly is still considered to be difficult [10–13]. Currently, some investigations have been focused on preparing core-shell nanoparticles with insulated shell that can restrain conductive particles from interconnecting. Liang et al. modified the surface of silver nanoparticles to form core-shell structured Ag@SiO₂ and then add them into BaTiO₃/poly(vinylidene fluoride)(PVDF) matrix. The permittivity of this resultant three-phase composites achieves 723 while remaining the dielectric loss of 0.82 at 100 Hz [14].

In this study, we present a CB@TiO₂/BaTiO₃/epoxy three-phase composites with higher dielectric constant than BaTiO₃/epoxy two-phase nanocomposites obtained by a similar technique. Epoxy resin was chosen as the polymer

✉ Zewei Li
g96217@scut.edu.cn

¹ School of Materials Science and Engineering, South China University of Technology, Guangzhou 510641, People's Republic of China

matrix because it is a kind of excellent insulating material that applied widely in the field of electronic manufacturing due to its excellent insulating property, strong ability of adhesion and anti-moisture, chemical stability and processing flexibility with printed circuit boards [15, 16]. Moreover, BaTiO₃ was chosen as the ferroelectric filler mainly because of its high permittivity which contributes to its extensive application in electrical engineering [17, 18].

Among various conductive fillers, carbon black (CB) is especially attractive because of its excellent conductivity, low cost and friendliness of environmental protection [19]. With a small content of CB adding into the ferroelectric-polymer composites, the permittivity of the obtained composites can realize an enhancement. That is the reason why carbon black was chosen as the conductive filler for the three-phase nanocomposites. Nevertheless, as mentioned above, the dielectric loss is critical for preparing composites with satisfactory dielectric performance. In present work, a semi-conductive TiO₂ layer is formed on the surface of the CB particles via a wet chemical method. It is assumed that the TiO₂ layer can avoid the interconnection of CB nanoparticles and act as a barrier layer to prevent the movement of free charge carriers thus suppressing dielectric loss.

The target of this investigation was to examine the effect of CB@TiO₂ nanoparticles and the TiO₂ layer on the dielectric performance of CB@TiO₂/BaTiO₃/epoxy composites system. The experimental results would be helpful for the improvement of high-k dielectric composites in the field of electronic packaging.

2 Experimental

2.1 Materials

Epoxy (bisphenol A epoxy resin, type E-44) used in this study was purchased from Guangzhou Dongfeng Chemical Industrial Cooperation Limited. Barium titanate particles with a grain size of 600 nm were supplied by Guangdong Fenghua Advanced Technology Holding Cooperation Limited. Carbon black was supplied by Cabot Chemical Cooperation Limited.

2.2 Sample preparation

2.2.1 Surface modification of the CB particles

Prior to being coated with TiO₂, carbon black particles were modified with HNO₃ to improve their dispersity in the ethanol solvent. The following procedure was used 5 g CB was dispersed in 150 mL HNO₃ solution (the mass fraction of HNO₃ was 65 wt%) under ultrasonic for 30 min. Then

the suspension was agitated mechanically at 80 °C. After 5 h, the achieved mixture was centrifuged. The obtained powder (denoted as H-CB) was washed by ultra-pure water and placed in a drying oven at 80 °C for 24 h.

2.2.2 Preparation of the CB@TiO₂ particles

The H-CB achieved above was dispersed in ammonia/ alcohol solution (the volume fraction of NH₃·H₂O was set at 0.3%) and ultrasonically agitated for 30 min followed by an addition of 1.2 mL tetrabutyl titanat (TBOT). Then the mixture was mechanically stirred at 45 °C. After 12 h, the CB@TiO₂ powder was collected by centrifugation and then washed with ethanol and dried to remove the residue.

2.2.3 Surface modification of BaTiO₃

KH550 was used for surface treatment of the BaTiO₃ particles. The content of KH550 was 1.5% by weight (wt%) of BaTiO₃ amount. The detailed procedure refers to the literature [20].

2.2.4 Preparation of the CB@TiO₂/BaTiO₃/epoxy thin film

Figure 1 presents the steps of preparation of the CB@TiO₂/BaTiO₃/epoxy thin film. Firstly, the epoxy resin was dissolved into the butanone followed by the addition of BT powder which was modified by surfactant (KH550) in order to enhance its compatibility in the epoxy matrix. The volume fraction of BT was 30%. Ultrasonic agitation was used for 25 min to improve the dispersion of BT powder by breaking its agglomeration. Secondly, the CB@TiO₂ powder was added into the as-prepared mixture and then ultrasonically agitated for 30 min and then stirred at 60 °C for 1 h. Thirdly, the curing agent (pyromellitic dianhydride, PMDA) was added into the suspension at a ratio of 40:100 by weight (curing agent:epoxy). With the volatilization of the butanone solvent, the mixture became more viscous and has a form of a slurry. Finally, achieved pulp was coated on the copper substrate by scratch coating and cured at a

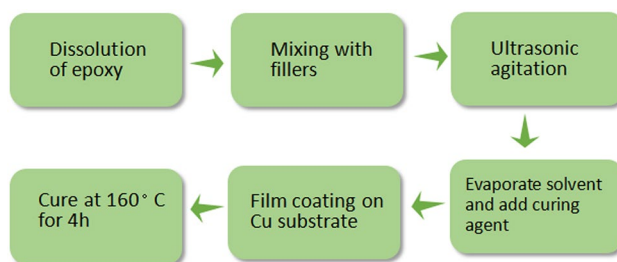


Fig. 1 Schematics of fabrication processes of CB@TiO₂/BaTiO₃/Epoxy composites thin film

temperature 160 °C for 4 h. Conductive silver paste was applied on the surface of the film as the top electrode.

2.3 Characterization

The microstructures of the CB@TiO₂ particles and the surface of the three-phase composites were observed by scanning electron microscopy (SEM; Nova Nano SEM 430). And the core-shell structure of the particles was investigated by transmission electron microscopy (TEM; JEM-2100HR). Fourier Transform Infrared (FTIR) spectra obtained by a FTIR Spectrometer (Vector33) were applied to detect functional groups on unmodified and KH550 modified BaTiO₃ particles. Dielectric properties were measured by an Agilent 4294 A impedance analyzer in the frequency range from 1 kHz to 1 MHz at room temperature.

3 Results and discussion

3.1 Morphology of CB@TiO₂ particles

Figure 2 shows the morphology of the CB@TiO₂ core-shell particles. From Fig. 2(a), it is found that the synthesized CB@TiO₂ particles grouped into agglomerates which consisted of lots of particulates. Such an observation mainly resulted from the conglomeration of the primary particles of CB. The spherical primary particulates of CB tend to melt into larger aggregates (usually bigger than 1 μm) due to their large surface area and massive functional groups on the surface. In other words, the core of CB@TiO₂ core-shell particles is the coacervate of CB. In addition, it is observed that some nanoparticles

appeared on the surface of aggregates (Fig. 2b) which are considered to be TiO₂.

The transmission electron microscopy (TEM) image of the CB@TiO₂ particles illustrates the core-shell structure. As shown in Fig. 3, a stable and dense amorphous titanium dioxide shell was directly observed on the surface of CB particles and the shell thickness is 10–20 nm. The result demonstrates that TiO₂ has been successfully deposited onto the surface of the CB.

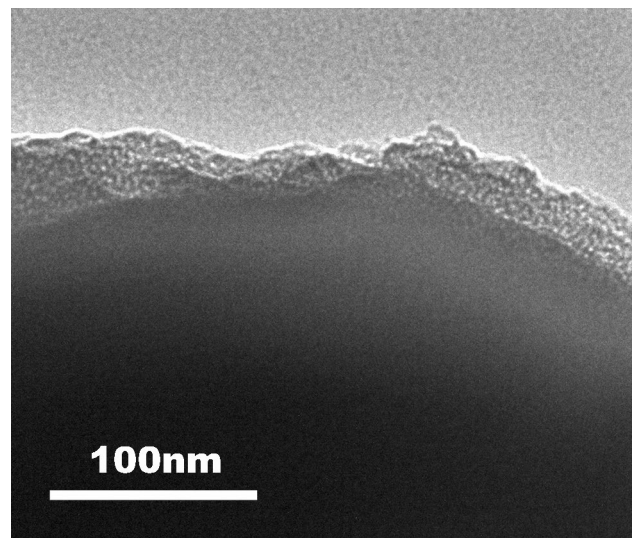


Fig. 3 TEM micrograph of CB@TiO₂ particles

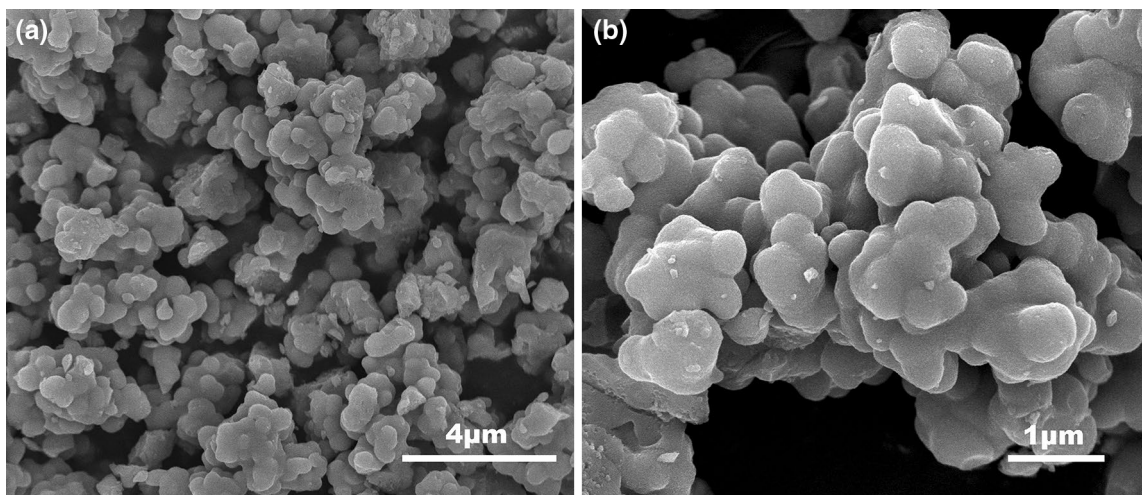


Fig. 2 SEM micrograph of CB@TiO₂ particles (magnifications of ×20, 000 was used for (a), and ×50, 000 for (b))

3.2 Dielectric properties of BaTiO₃/Epoxy composites

3.2.1 FTIR analysis on BaTiO₃ modified by KH550

Figure 4 shows the FTIR spectra of pristine BaTiO₃ and BaTiO₃ particles modified by KH550. It is observed that BaTiO₃ treated by KH550 has absorption peaks at 2922 and 2858 cm⁻¹, assigned to asymmetric stretching vibration of methylene and symmetric stretching vibration of methylene, respectively [21–23]. Additionally, compared with the spectra of pure BaTiO₃ particles, mixture of BaTiO₃ and KH550 displays a new absorption band at 1085 cm⁻¹ which is the characteristic peak of Si–O–C group from KH550. Hence, chemical adherence of KH550 to the surface of BaTiO₃ can be confirmed [24].

3.2.2 Effect of BaTiO₃ loading on BaTiO₃/Epoxy composites

Figure 5 presents the variation of permittivity of BaTiO₃/Epoxy two-phase composites with different volume fraction of the BaTiO₃ content at the frequency of 100 kHz. A gradual increment in dielectric constant with BaTiO₃ loading can be observed in the composites. The increase in dielectric constant of BaTiO₃/Epoxy two-phase composites is mainly due to higher permittivity of BaTiO₃ (1200 at 100 kHz) compared to epoxy resin (2.9 at 100 kHz). Moreover, more interfaces of the epoxy matrix and BaTiO₃ ceramic appear in the composite and hence interfacial polarization is strengthened, which lead to higher dielectric constant of the BaTiO₃/Epoxy composites. Therefore, the content of BaTiO₃ in the composites is a necessary factor in improving permittivity of the composites. However, a limitation of BaTiO₃ content is existing for BaTiO₃/Epoxy

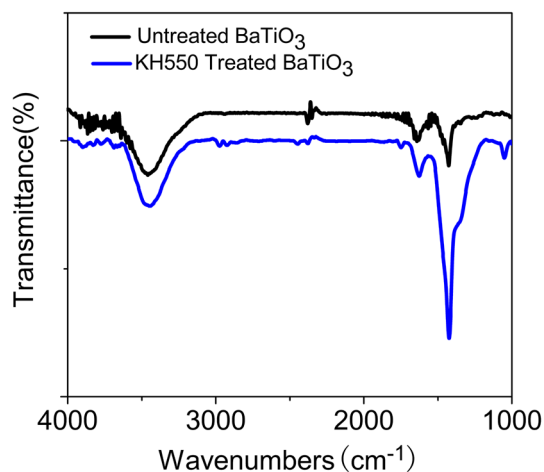


Fig. 4 FTIR spectra of pristine BaTiO₃ and BaTiO₃ particles modified by KH550

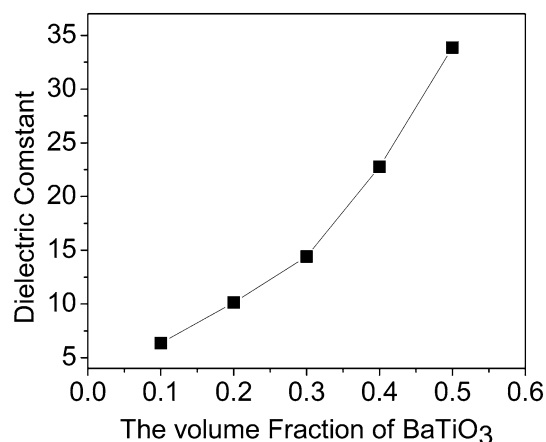


Fig. 5 Dielectric constant of BaTiO₃/Epoxy composites (at 100 kHz)

two-phase composites to enhance its dielectric properties. Reports show that more defects begin to emerge in the composites when the BaTiO₃ loading is more than 30 vol% thus leading to lower breakdown strength [25]. Hence, in this study, epoxy with 30 vol% BaTiO₃ is considered for further studies to investigate the effect of CB@TiO₂ fillers on the dielectric properties of CB@TiO₂/BaTiO₃/Epoxy three-phase composites.

3.3 Dielectric properties of CB@TiO₂/BaTiO₃/Epoxy composites

3.3.1 Dielectric constant of CB@TiO₂/BaTiO₃/Epoxy composites

Figure 6 shows the frequency dependence of dielectric constant of CB@TiO₂/BaTiO₃/Epoxy composites. A gradual decrease in dielectric constant with frequency is observed for all the composites. This is expected since polarization

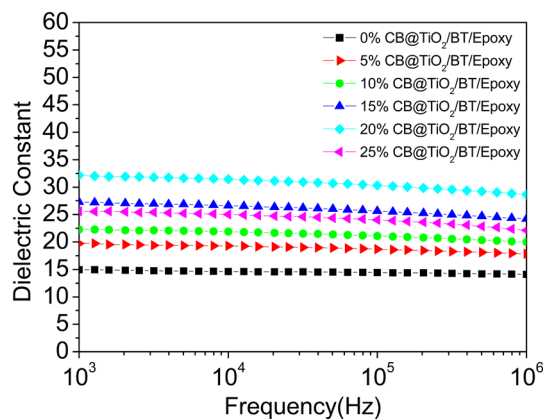


Fig. 6 Frequency dependence of dielectric constant of the CB@TiO₂/BaTiO₃/Epoxy composites

mechanisms are frequency dependent, the intensity of polarization usually decrease with an increasing frequency. At the range of 1 kHz–1 MHz, the polarization in CB@TiO₂/BaTiO₃/Epoxy composites is mainly built by the carriers at the interfaces between each two different inclusions. Therefore, the gradual reduction of permittivity with frequency is due to the decreasing intensity of interfacial polarization [26]. In addition, it can be observed that CB@TiO₂/BaTiO₃/Epoxy composites with high loading fraction of CB@TiO₂ has a greater dielectric constant. The permittivity of the CB@TiO₂/BaTiO₃/Epoxy three-phase composites with 20 vol% of CB@TiO₂ filler reaches 32.14 at the frequency of 1 kHz, in contrast to 14.96 for the BaTiO₃/Epoxy two-phase composites. However, when the content of CB@TiO₂ reaches 25%, the dielectric constant drops to 25.57 in 1 kHz.

The present CB@TiO₂/BaTiO₃/Epoxy composites can be considered as the loading of conducting CB particle in the insulating BaTiO₃/Epoxy phase. Figure 7 presents both experimental and theoretical values of relative dielectric constant of CB@TiO₂/BaTiO₃/Epoxy composites with different volume fraction of CB@TiO₂ at 1 MHz. The filler content dependence of dielectric constant is given by the following power law on the basis of percolation theory [27]:

$$\epsilon(V) = \epsilon_0 \left(\frac{V_c - V}{V_c} \right)^{-q}$$

where ϵ_0 is the permittivity of BaTiO₃/Epoxy composites, V_c is the volume fraction of CB@TiO₂ at percolation, V is the volume fraction of CB@TiO₂ and q is a critical exponent. The experimental values of dielectric constant

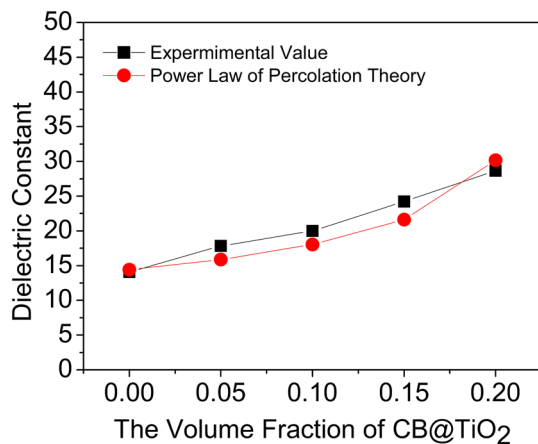


Fig. 7 Dielectric constant of CB@TiO₂/BaTiO₃/Epoxy composites with different volume fraction of CB@TiO₂ below the percolation threshold and the comparison with power law

are in agreement with the equation, with $V_c = 24.1$ vol%, $q = 0.41662$.

3.3.2 Dielectric loss of CB@TiO₂/BaTiO₃/Epoxy composites

Figure 8 shows the frequency dependence of dielectric loss of CB@TiO₂/BaTiO₃/Epoxy composites. It can be observed that the dielectric loss of all composites increase gradually with the increasing frequency. This is also caused by the frequency dependent of the polarization. The establishment of polarization in the composites requires a certain period. When this period is shorter than the period of the electric field variation, the direction of polarization cannot keep up with the variation of electric field, which leads to the relaxation of polarization in the composites. It can be concluded that the relaxation of interfacial polarization strongly affects the dielectric loss of CB@TiO₂/BaTiO₃/Epoxy composites. Additionally, as shown in Fig. 8, composite films with CB@TiO₂ keep higher dielectric loss than BaTiO₃/Epoxy two-phase composites. Moreover, composites with 25 vol% of CB@TiO₂ filler show a highest dielectric loss among composites with different CB@TiO₂ filler content.

3.3.3 Conductivity of CB@TiO₂/BaTiO₃/Epoxy composites

Figure 9 presents the frequency dependence of conductivity of CB@TiO₂/BaTiO₃/Epoxy composites. As the CB@TiO₂ filler loading increased, the conductivity of the composite film also increased. This could be described to the introduction of more interfaces by the CB@TiO₂ particles. The space charge tends to accumulate at the interfaces between different components. These carriers are considered to contribute to the leakage current by the influence of electric field. Therefore, the increasing conductivity is mainly

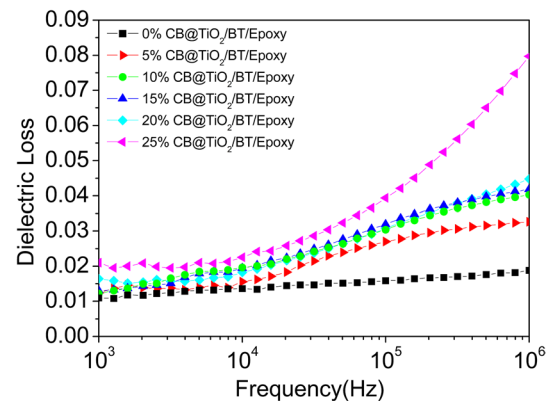


Fig. 8 Frequency dependence of dielectric loss of the CB@TiO₂/BaTiO₃/Epoxy composites

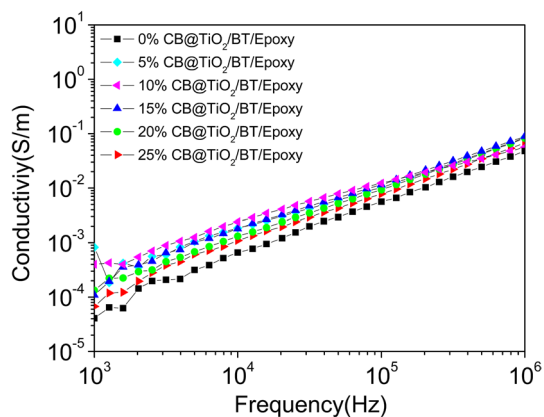


Fig. 9 Frequency dependence of conductivity of the CB@TiO₂/BaTiO₃/Epoxy composites

attributed to the increase of the leakage current caused by the carriers at the interfaces.

3.3.4 Morphology of CB@TiO₂/BaTiO₃/Epoxy composites

The morphology of the surface of CB@TiO₂/BaTiO₃/Epoxy composites is shown in Fig. 10. We can see that the surface of three-phase composite film which has 5 vol% CB@TiO₂ filler (Fig. 10a) is relatively smooth. Most of filler particles are coated with epoxy and only a few particles can be observed by SEM. In contrast, composites film with 25 vol% CB@TiO₂ filler loading keeps a rough surface. Massive particles reunite and pile up so that they can be discerned even though they are covered by epoxy. Therefore, the deterioration of dielectric properties of the composites with 25 vol% CB@TiO₂ filler can be attributed to the relatively more pores which brought by the higher

loading of CB@TiO₂ filler (Fig. 10b). In other words, excessive volume of CB@TiO₂ filler in the composites leads to a greater probability of particle aggregation [28].

3.3.5 Effect of the BaTiO₃ loading on the dielectric properties of CB@TiO₂/BaTiO₃/Epoxy composites

In order to further confirm the effect of the BaTiO₃ loading on the dielectric properties of CB@TiO₂/BaTiO₃/Epoxy composites, CB/BaTiO₃/Epoxy composites which filled with 25 vol% CB@TiO₂ and BaTiO₃ was prepared. Figure 11 shows the variation of dielectric constant and dielectric loss of 25% CB@TiO₂/BaTiO₃/Epoxy composites with different volume fraction of BaTiO₃ at the frequency of 100 kHz. The dielectric constant of the composites is found to increase with the BaTiO₃ loading. It is predictable

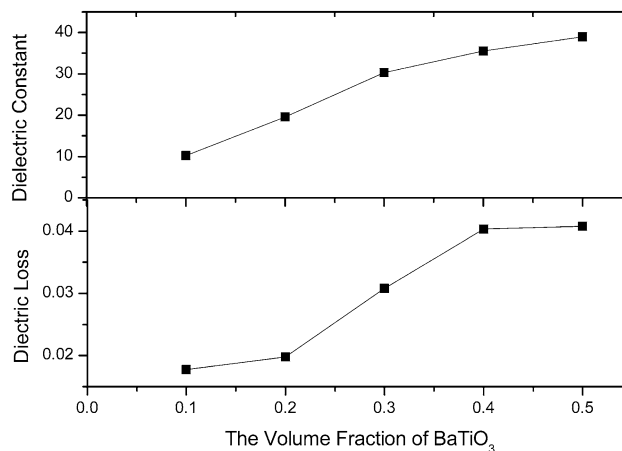


Fig. 11 Dielectric constant and dielectric loss of 25%CB@TiO₂/BaTiO₃/Epoxy composites (at 100 kHz)

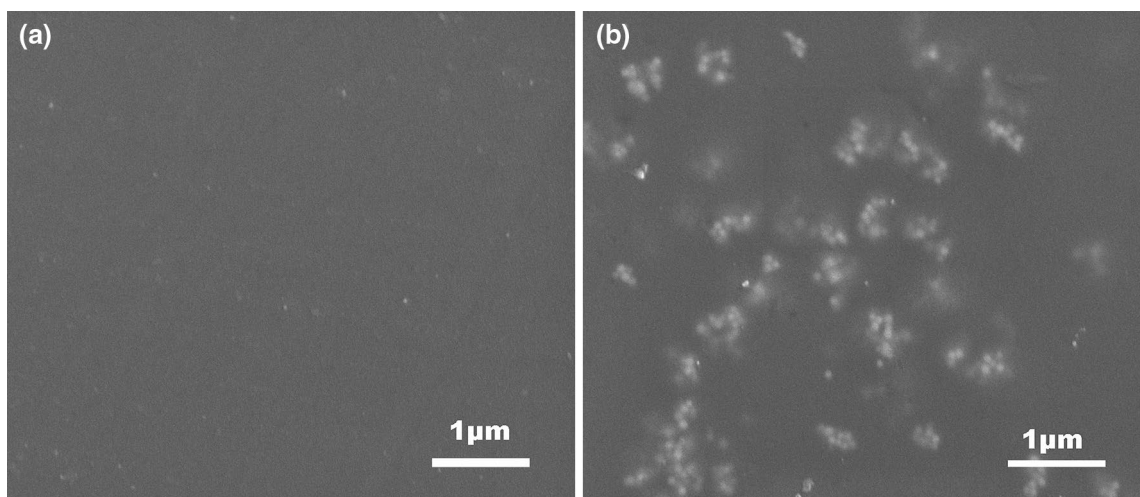


Fig. 10 SEM images of the CB@TiO₂/BaTiO₃/Epoxy composites with **a** 5 vol% CB@TiO₂ and **b** 25 vol% CB@TiO₂

because increasing content of BaTiO₃ in the composites is helpful in enhancing the dielectric constant of the composites. On the other hand, a gradual increase in dielectric loss with the volume fraction of BaTiO₃ is also observed in the composites. Higher loading of BaTiO₃ in the composite introduces more interface between BaTiO₃ and polymer, more defects also emerge in the meantime thus leading to a higher dielectric loss of the composites. It is necessary to control the content of BaTiO₃ in the composites appropriately.

3.3.6 Effect of the TiO₂ shell on the dielectric properties of CB@TiO₂/BaTiO₃/Epoxy composites

To further investigate the effect of the TiO₂ shell on the dielectric properties of CB@TiO₂/BaTiO₃/Epoxy composites, CB/BaTiO₃/Epoxy composites which filled with pristine CB were fabricated. Frequency dependences of dielectric properties of CB/BaTiO₃/Epoxy composites and CB@TiO₂/BaTiO₃/Epoxy composites are depicted in Fig. 12. Both of these two groups of investigated three-phase composites contain the same volume of CB fillers (5 vol%) and BaTiO₃ (30 vol%). As shown in Fig. 12, composites with CB@TiO₂ filler keep higher permittivity than that with uncoated CB while the dielectric loss of the former is much lower. The reason for this can be considered with the characteristics of titanium dioxide and interface polarization effect. Titanium dioxide exhibited higher dielectric constant than pristine CB, thus leading to a greater permittivity of CB@TiO₂. Moreover, the TiO₂ shell shows a more intense interaction with the epoxy matrix and creates an interphase which has massive space charges. Stronger interface polarizability can be built at the interfaces so that higher dielectric constant originates [14, 29]. In addition, some of the uncoated CB particles dispersed in the epoxy

matrix are liable to agglomerate into larger aggregates. These particles contact with each other and then result in a tendency to form conductive paths in the composites. Free charge carriers can move through these conductive paths by the influence of an electric field and then enhance the leakage current. So the conduction loss which is enhanced by leakage current is considered as a reason for the increasing dielectric loss of the composites [8]. By comparison, CB@TiO₂ particles have a semiconductor shell which can prevent directly contact between CB particles. Therefore, CB@TiO₂ particles are less likely to form conductive paths even they are reunited. It can be concluded that the TiO₂ shell of CB@TiO₂ particles not only improve the dielectric constant but also plays an important role in reducing the dielectric loss of the composites.

4 Conclusions

CB@TiO₂ core-shell particles were successfully prepared by a wet chemical method and their incorporation with BaTiO₃/epoxy three-phase composites shows an improvement of the dielectric properties of the composites. The dielectric constant of the composites increases with the concentration of the CB@TiO₂ until the content reaches 25% due to the higher probability of particle aggregation. Therefore, the CB@TiO₂/BaTiO₃/Epoxy composites with the dielectric constant of 32.14 at 1 kHz remain low dielectric loss (0.016 at 1 kHz) is fabricated. Besides that, the TiO₂ semiconductor shell on the surface of conductive CB particles plays an important role in improving the dielectric properties of the composites because it can create isolation between CB particles. The results indicated in this study demonstrate that CB@TiO₂/BaTiO₃/Epoxy composites is

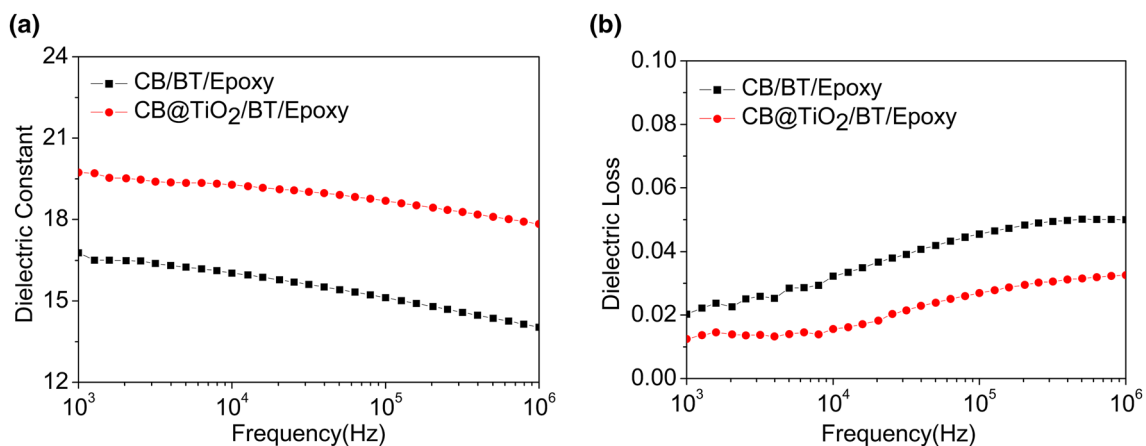


Fig. 12 Frequency dependence of **a** dielectric permittivity and **b** dielectric loss of the CB@TiO₂/BaTiO₃/Epoxy composite and CB/BaTiO₃/Epoxy composite

suitable to be employed in embedded capacitors and energy storage systems.

References

1. D.S. Kim, C. Baek, H.J. Ma, D.K. Kim, *Ceram. Int.* **42**, 7141 (2015)
2. V. Pascariu, O. Avadanei, P. Gasner, I. Stoica, A.P. Reverberi, L. Mitoseriu, *Phase Transit.* **86**, 715(2013)
3. S. Jayanthi, A. Arulsankar, B. Sundaresan, *Appl. Phys. A* **122**, 22 (2016)
4. M.S.D. Satia, M. Jaafar, *J. Appl. Polym. Sci.* **133**, 43313 (2016)
5. T. Li, J. Chen, H.Y. Dai, D.W. Liu, H.W. Xiang, Z.P. Chen, *J. Mater. Sci.* **26**, 312 (2015)
6. J. Su, J. Zhang, *J. Mater. Sci.* **27**, 4344 (2016)
7. Z.M. Dang, M.S. Zheng, J.W. Zha, *Small* **12**, 1688 (2016)
8. S. George, M.T. Sebastian, *Compos. Sci. Technol.* **69**, 1298 (2009)
9. B. Mathieu, C. Anthony, A. Arnaud, F. Lionel, *J. Mater. Chem. C* **3**, 5769 (2015)
10. A.L. Santos, E.C. Botelho, K.G. Kostov, M. Ueda, L.L.G. da Silva, *Adv. Mater. Res.* **1135**, 75(2012)
11. B.H. Wang, L.M. Liu, L.Z. Huang, L.F. Chi, G.Z. Liang, L. Yuan, A.J. Gu, *Carbon* **85**, 28 (2015)
12. A. Qajar, M. Peer, M.R. Andalibi, R. Rajagopalan, H.C. Foley, *Microporous Mesoporous Mater.* **218**, 15(2015)
13. C.L. Poh, M. Mariatti, A.F.M. Noor, O. Sidek, T.P. Chuah, S.C. Chow, *Compos. Part B-Eng.* **85**, 58(2015)
14. X.W. Liang, S.H. Yu, R. Sun, S.B. Luo, J. Wan, *J. Mater. Res.* **27**, 991 (2012)
15. S. Paul, T.K. Sindhu, *IEEE Trans. Dielectr. Electr. Insul.* **21**, 2164 (2014)
16. H.G. Lee, K.W. Paik, *IEEE Trans. Compon. Packag. Manuf. Technol.* **5**, 451 (2015)
17. Z.M. Dang, J.K. Yuan, J.W. Zha, T. Zhou, S.T. Li, G.H. Hu, *Prog. Mater. Sci.* **57**, 660 (2012)
18. Y.Q. Wu, J.L. Zhang, Y.Q. Tan, P. Zheng, *Ceram. Int.* **42**, 9815(2016)
19. Y.R. Smith, D. Bhattacharyya, T. Willhard, M. Misra, *Chem. Eng. J* **396**, 102 (2016)
20. J. Su, S. Chen, J. Zhang, Z. Xu, *Polym. Test* **28**, 419 (2009)
21. M. Tian, W.L. Liang, G.Y. Rao, L.Q. Zhang, C.X. Guo, *Compos. Sci. Technol.* **65**, 1129 (2005)
22. C. Nakason, P. Wannavilai, A. Kaesaman, *Polym. Test* **25**, 34 (2006)
23. S. Pongdhorn, S.B. Chakrit, K. Hatthapanit, U. Thepsuwan, *Polym. Test* **24**, 439 (2005)
24. F. Chao, L.G. Liang, *J. Mater. Sci.* **20**, 560 (2009)
25. Z.F. Zhang, X.F. Bai, J.W. Zha, W.K. Li, Z.M. Dang, *Compos. Sci. Technol.* **115**, 87 (2012)
26. P. Chylek, V. Srivastava, *Phys. Rev. B* **1008**, 30 (1984)
27. A.L. Efors, B.I. Shktovskii, *Phys Status Solidi B* **477**, 76 (1976)
28. Z.F. Zhang, X.F. Bai, J.W. Zha, W.K. Li, Z.M. Dang, *Compos. Sci. Technol.* **97**, 102 (2014)
29. M. Rahimabady, M.S. Mirshekarloo, K. Yao, L. Lu, *Phys. Chem. Chem. Phys.* **15**, 16245 (2013)